Enhancing the Number of High-Energy Electrons Deposited to a Compressed Pellet via Double Cones in Fast Ignition

Hong-bo Cai,[1,*] Kunioki Mima,[1,†] Wei-min Zhou,[1] Tomoyuki Jozaki,[1] Hideo Nagatomo,[1]
Atsushi Sunahara,[1] and Rodney J. Mason[2]

[1]*Institute of Laser Engineering, Osaka University, 2-6 Yamadaoka, Suita, Osaka 565-0871, Japan*
[2]*Research Applications Corporation, Los Alamos, New Mexico 87544, USA*

Particle-in-cell simulations aimed at improving the coupling efficiency of input laser energy deposited to a compressed core by using a double cone are described. It is found that the number of high-energy electrons escaping from the sides of the cone is greatly reduced by the vacuum gap inside the wing of the double cone. Two main mechanisms to confine high-energy electrons are found. These mechanisms are the sheath electric field at the rear of the inner cone wing and the quasistatic magnetic field inside the vacuum gap. The generation mechanism for the quasistatic magnetic fields is discussed in detail. It is found that the quasistatic fields continue to confine the high-energy electrons for longer than a few picoseconds. The double cones provide confinement and focusing of about 15% of the input energy for deposition in the compressed core.

In the fast ignitor [1], a relativistic electron beam is considered to be the most suitable source for igniting a hot spot much smaller than the dense compressed deuterium-tritium core. Many experiments [2–4] have been carried out to study the feasibility of fast ignition with relativistic particles. One task is how to achieve efficient generation of enormous numbers of high-energy charged particles [5–7]. In order to improve the efficiency of the coupling and transport of the energy into dense plasma, cone targets [8,9] have been used in the fast ignition scheme. The merits of cone targets have been shown both in experiments [9] and simulations [7,10].

Several physics issues have to be examined before a realistic assessment of this method can be made. Among these issues are the control and guidance of the high-energy electrons to the cone tip. As is well known, the cone target is surrounded by a coronal plasma generated by the implosion of a fuel capsule. The radiation hydrocode PINOCO [11] shows that coronal plasma density is well above the critical density. In this case, electrons accelerated by the laser field can escape freely from cone sides to the surrounding coronal plasma, resulting in the decrease of the energy flux through the cone tip. Nakamura *et al.* [10] have suggested a double cone to prevent the electrons from escaping aside. Their results show that the double cone confines the electrons for hundreds of femtoseconds with an immobile ion background. In their simulations the electrons are blocked by the sheath electric field inside the vacuum gap. However, the plasma expansion could be very significant for picosecond time scale simulations, since the ions are accelerated into the vacuum gap by the electrostatic fields. Over several hundreds of femtoseconds the sheath electric field inside the gap could be reduced to a very low level. Therefore, important questions are (1) whether the double cone is still effective in confining

the high-energy electrons after one picosecond and (2) how much energy can be confined and focused to the compressed core by using the double cone? These are the principal subjects of this Letter.

Here we present some results from 2.5D simulations using the particle-in-cell (PIC) framework ASCENT (assembly system for computational experiment) developed in ILE, Osaka University. Figure 1(a) is a sketch of the geometry of the simulations. In our double cone target the inner cone wall is isolated from the background plasma (corona plasma) due to a vacuum gap. The width of our inner cone wing is $5\lambda_0$ and the width of the gap is $3\lambda_0$. The
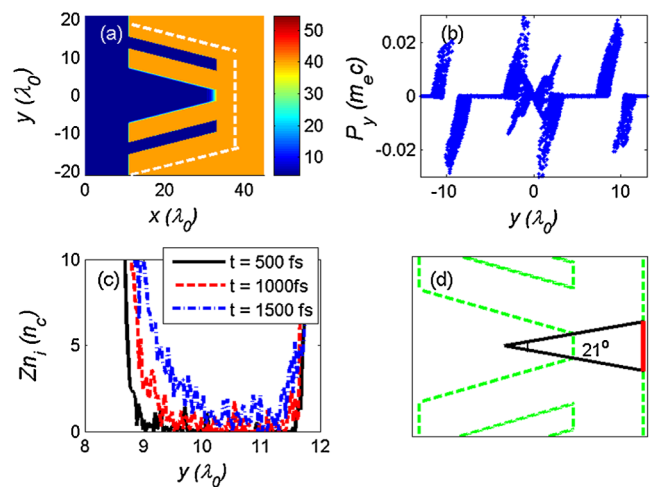

FIG. 1 (color online).   (a) Initial density profile of the double cone target. (b) Phase space of high Z ions in the region $x \in (25, 30)\lambda_0$ at $t = 500$ fs. (c) A slice of the ion density profile at position $x = 25\lambda_0$ inside the upper gap of the double cone target. (d) Sketch of collection cone (dark) for the double cone target (green dashed line).

plasma consists of three species: electrons, protons with $m_p/m_e = 1836$ outside the cone, and heavy ions (gold ion with an assumed charge state $Z_i = 40$) and $m_i/m_e Z_i = 195.4/40$, where $Z_i = 40$ corresponds to the average ionization state of the gold at 1 keV temperature. The gold cone, whose edge is drawn with the white dashed lines, is surrounded by a hydrogen plasma. Both the plasma density of the gold cone and that of the hydrogen plasma are $40n_c$. The p-polarized laser pulse at $\lambda_0 = 1.06$ μm wavelength and 1.2×10^{19} W/cm^2 intensity irradiates the target from the left boundary. The intensity profile is Gaussian in the y direction with a spot size of 5.0 μm (FWHM). The laser rises in $20T_0$, where T_0 is the laser period, after which the laser amplitude is kept constant. A typical simulation duration is $450T_0$, which corresponds to about 1.5 ps for $\lambda_0 = 1.06$ μm.

Here, we use a grid size of $\Delta x = \Delta y = \lambda_0/64$ with 2800×2688 grid cells. The time step used is $0.01T_0$. Fifty particles are used in one mesh, and the total number of particles is about 2.55×10^8. Both the field and particle boundary conditions are absorbing boundary conditions, either in the x or the y direction. Over the current simulation time scale (picoseconds), a large number of high-energy electrons escaping to the boundaries are reflected back by a large unphysical sheath field generated there. In order to eliminate this sheath field, we set cooling buffers at the boundaries in our simulation. Furthermore, in order to reduce the restrictions on the grid size compared with the Debye length, we used a fourth-order interpolation scheme to evaluate fields and currents.

Crucial issues for the fast ignitor are the generation and transport of enormous numbers of high-energy electrons to the compressed core. The mechanism here proposed for transverse confinement of the high-energy electrons relies on the fact that in the double cone targets the inner cone is isolated from the corona plasma by a vacuum gap. The most familiar example of this effect is the sheath electric fields set up at the rear side of an inner cone [6,10]. However, on picosecond time scales, we found that the mechanisms to confine high-energy electrons are different.

To determine the plasma expansion inside the gap, we plot the phase space of high Z ions in the region $x \in (25, 30)\lambda_0$ at time $t = 500$ fs in Fig. 1(b). Notice that the ion velocity can reach as high as $0.01c$. Therefore, after 1 ps, even the high Z ions can move as far as $3\lambda_0$. Note that the width of the vacuum gap inside the cone wing is only $3\lambda_0$ and the plasma expansion occurs at both sides of the gap. Figure 1(c) shows the time evolution of the ion density inside the gap. Clearly, after 1 ps of interaction the vacuum gap is filled with plasma density that can be as high as several critical densities. Thus, we may conclude that we cannot expect the sheath electric fields to still be effective in confining high-energy electrons after $t > 1$ ps, as shown in Figs. 2(a) and 2(b).

In Fig. 3 the energy density distributions of electrons with energy between $0.5 \leq E$ [MeV] ≤ 2.0 are plotted. It
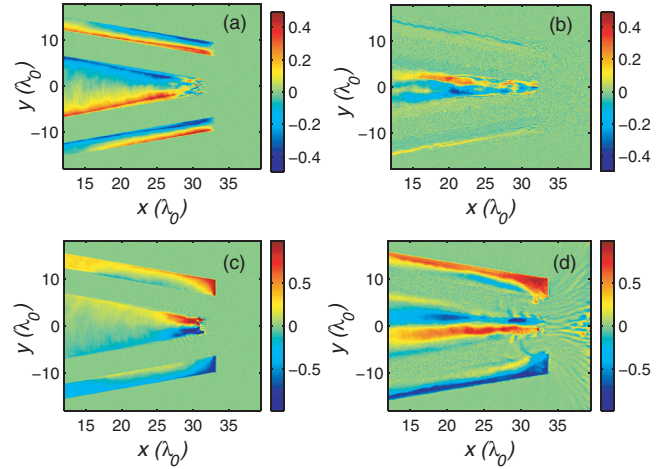

FIG. 2 (color). (a),(b) The sheath electric fields at time (a) $t = 330$ fs and (b) $t = 1500$ fs. (c),(d) The quasistatic magnetic fields at time (a) $t = 330$ fs and (b) $t = 1500$ fs. Here, both the sheath electric fields and the quasistatic magnetic fields are averaged over one laser period. The unit of the electromagnetic (EM) fields is $m_e\omega_0 c/e$ (1 unit = 100 MG for magnetic field).

is clearly seen that the high-energy electrons are mainly accelerated at the cone tip and cone sidewall. In the single cone case, some of the high-energy electrons move freely into the surrounding corona plasma and then the energy flux decreases through the cone tip. Alternatively, in the double cone case, few electrons can "leak" out into the surrounding corona plasma even after 1 ps. But remember that Fig. 2(b) shows that the sheath electric fields have already decreased to a very low level at later times. What then is the active longer time mechanism for blocking the high-energy electrons?

Figure 4(a) is the plot of the maximum values of the quasistatic magnetic field and sheath electric field inside the gap. These results show that the sheath electric field peaks at time $t = 250$ fs, and eventually decreases to a very low level after time $t = 600$ fs. In comparison, the quasistatic magnetic field still keeps growing after it grows up at time $t = 330$ fs. It is important to stress that the gyroradius of a typical 1 MeV hot electron is less than $\lambda_0/2$ under the quasistatic magnetic fields which are the
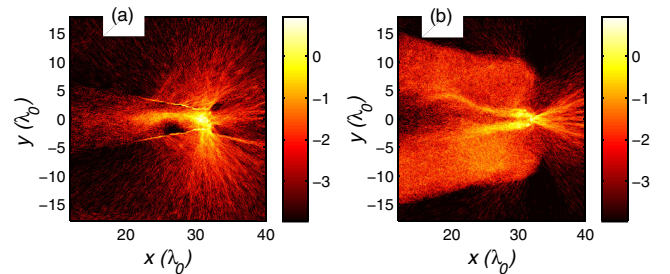

FIG. 3 (color online). The natural logarithm of the electron energy density for single cone (a) and double cone (b) at time $t = 1000$ fs. Here the electron energy density is normalized by $m_e c^2 n_c$.

order of 100 MG. Therefore, the electrons escaping into the vacuum gap can be effectively reflected back by the magnetic fields.

Various nonlinear mechanisms have been invoked to explain the generation of quasistatic magnetic fields [12–14], but inside the "vacuum" gap, the most plausible mechanism is principally due to a localized supply of high-energy electrons, originally produced at the inner cone side and cone tip. We notice that there are two oppositely directed currents in the gap, as shown in Fig. 4(b). The positive one is mainly produced by the high-energy electrons coming from the cone tip, while the negative one is a surface current moving along the inner surface of the outer cone. The collaboration of these two currents can therefore give rise to a large quasistatic magnetic field inside the gap, as shown in Figs. 2(c) and 2(d).

The reason for the first rapid increase of magnetic field inside the gap [as shown in Fig. 4(a)] is simple: the high-energy electron current increases with the rise of the incident laser amplitude. Of particular importance to fast ignition is that the magnetic field still keeps growing after the laser amplitude reaches its maximum. The physics of the growth of the quasistatic magnetic field is straightforward. Consider a relativistic laser pulse irradiating a double cone. Since some high-energy electrons escape into the cone gap, a high-energy electron current $\mathbf{J}_h = -en_h\mathbf{v}_h$ is generated inside the gap. This high-energy electron current is seeding the magnetic field $\langle B_z \rangle$ inside the gap. But, at a later time, this current should be constant, since the input laser energy becomes constant. In turn, the magnetic field, together with the electric field, reflects the

high-energy electrons into the inner cone and the reflected electrons recirculate in the cone to generate an additional electric current J_P inside the gap. In order to evaluate the total energy of the recirculating high-energy electrons Q_h, we employ

$$\frac{dQ_h}{dt} = G - Q_h \frac{cS}{3V}(1 - \beta) - Q_h \frac{cS_0}{3V}, \qquad (1)$$

where G is the input laser energy, the second term is the energy flux escaping to the side, β is the reflectivity of high-energy electrons by the electromagnetic fields, S is the side area, V is the total volume of the system, and the third term is the energy flux emitted from the cone tip. Also, S_0 is the area of the cone tip. We assume $|d \ln \beta/dt| \ll \Omega \equiv cS/3V$, then integrate Eq. (1) to obtain

$$Q_h = \left\{ 1 - \exp\left[-\Omega\left(\int_0^t (1 - \beta(t))dt + tS_0/S \right) \right] \right\}$$
$$\times \frac{G}{\Omega[(1 - \beta) + S_0/S]}. \qquad (2)$$

Equation (2) indicates that the total energy of high-energy electrons increases with time. As a numerical example, we evaluate Eq. (2) for the present double cone case. According to Fig. 3(b), the cone tip area S_0 is about 10 μm and the side area S is about 40 μm. On the other hand, the flux escaping from the sidewall is about 1/4 of the flux escaping from the tip (it will be shown in Table I). Those facts indicate that $(1 - \beta)$ is about 1/16. Since $V \simeq 500$ μm^2, $\Omega \equiv cS/3V = 8 \times 10^{12}$ s^{-1}. So that the electron accumulation time, $\tau_a = [d \ln(Q_h)/dt]^{-1}$, can be estimated as $\tau_a = [\Omega(1 - \beta) + S_0/S]^{-1} \sim 0.5$ ps. Then $Q_h(t)$ of Eq. (2) is plotted in Fig. 4(a) (note that there is a delay in generating the high-energy electrons). This indicates that the quasistatic magnetic field $\langle B_z(t) \rangle$ is proportional to $Q_h(t)$. By taking into account Ampère's law, $\nabla \times \langle B_z \rangle \approx 4\pi(J_h + J_P)/c$, it is concluded that $J_P \propto Q_h$ when J_P is dominant. The reason why J_P is proportional to Q_h is as follows: some of the high-energy electrons are bounced back and forth inside the inner surface of the cone wing by the magnetic fields, which results in the rapid increase of the high-energy electron density inside the inner cone wing. As a result, the pressure gradient builds up on the inner surface of the outer cone wing to generate the diamagnetic current $\mathbf{J_P}$, as shown in Fig. 4(b). It is worth stressing that we can expect from these equations that at a later time when the magnetic field increases to a
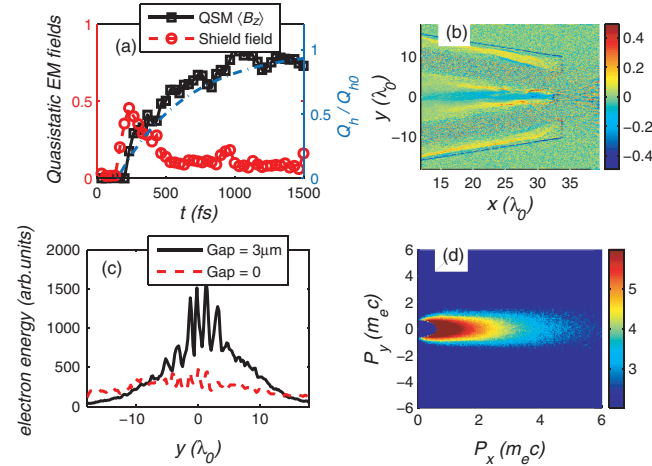

FIG. 4 (color). (a) The maximum values of the quasistatic magnetic field (QSM, solid line) and the sheath electric field (dashed line) inside the gap. The measured data are the average of three slices at $x = 24$, 25, and 26λ_0. The units of the EM fields are $m_e\omega_0 c/e$. The dash-dotted line is the plot of $Q_h(t)$ in Eq. (2). (b) The time averaged current j_x (over one laser period) at time 1500 fs. (c) The transverse distribution of the energy of the escaped electrons from the right boundary. (d) The natural logarithm of the momentum distribution of the collected high-energy electrons.

TABLE I. Fraction of the energy flux of the emitted high-energy electrons at different boundaries with respect to the input laser energy for double cone and single cone.

| | Right | | | | |
	$(-18, 18)\lambda_0$	21° cone	Down	Up	Left
Gap = 0	27.4%	4.8%	17.2%	13.0%	0.54%
Gap = 3	44.0%	14.8%	5.0%	6.4%	0.55%

high level, nearly all the injected high-energy electrons are reflected inside the gap, $\beta \to 1$, we then expect $Q_h \cong \frac{G}{\Omega S_0/S}$.

The fractions of energy flux of emitted high-energy electrons, defined as the ratio of the escaped electron kinetic energy from each boundary to the total input laser energy, are listed in Table I for the single cone target case and double cone case. Here, the escaped high-energy electrons are observed at the boundaries (before the cooling buffers). In the single cone target case only 47.6% of the total absorbed laser energy is contained in the forward energy flux by high-energy electrons. When using a double cone, this fraction can be as high as 79.4%. In fact, a significant amount of the high-energy electrons that escaped from the sidewalls—carrying about 19% of the total input laser energy—are saved for the double cone case as compared with that in the single cone case. Most of these saved high-energy electrons are transferred directly to the cone tip, which will contribute to heat the core of the fast ignition pellet. Another part of these high-energy electrons is contained inside the inner cone wing, resulting in the increase of the temperatures of the plasma inside the cone. At a later time this part of the energy will contribute to heat the core of the fast ignition pellet.

We next examine how the vacuum gap affects the forward high-energy electron flux. In Fig. 4(c) we plot the time-integrated electron energy observed at $x = 40\lambda_0$ as a function of the y coordinate. Because of the cone gap effects, the double cone shows a larger electron energy flux than the single cone, especially in the center of the cone target. It is also found that the focusing of the high-energy electrons becomes much better when using the double cone target. But still, only 20%–40% of the forward energy flux can heat the core. This is due to the large angular spread of the electrons emanating from the impact point. To determine the energy flux of electrons injected into the core, we measure the high-energy electrons across a series of planes within the cone that would hit a 10 μm radius hot spot [5], which is located several tens of microns away from the impact point. The sketch of the collection cone is shown in Fig. 1(d), whose collection cone angle is 21°. We found about 14.8% of input laser energy can deposit in the core. In Fig. 4(d) the momentum distribution of this group of collected electrons with energy larger than 100 keV shows that the double cone target works effectively in collimating and focusing high-energy electrons. Moreover, we observe that there are several stronger electron energy peaks in the double cone case. These peaks are due to the formation of filament due to the Weibel instability [15].

In summary, we performed 2.5D PIC simulations to study the merits of double cone in fast ignition. Our simulation results indicate that the energy flux through the cone tip in the double cone is much larger and more tightly focused than that in the single cone. It has been shown that in the single cone case, the high-energy electrons, about 30% of the total input laser energy, escape into the surrounding corona plasma from the sidewalls. In comparison, in the double cone case the high-energy electron flux, about 11% percent of the total input laser energy, escapes from the sidewalls. It is found that the 3 μm gap is enough to confine high-energy electrons and enhance the electron energy flux to the cone tip. In an actual target, both the size of the cone and the gap are larger. In this case, the electrostatic field inside the gap will confine for a longer time. Furthermore, the magnetic fields inside the gap are also expected to grow since, at the cone sides, there are always some group of escaped electrons, which together with the magnetic fields form a feedback loop inside the gap. Therefore, the high-energy electron confinement would be better for the larger scale cone than the present one, and the results presented in this Letter provide critical information needed to design an optimized cone target geometry.

*hongbo-cai@ile.osaka-u.ac.jp
†mima@ile.osaka-u.ac.jp

[1] M. Tabak *et al.*, Phys. Plasmas **1**, 1626 (1994).
[2] T. A. Hall *et al.*, Phys. Rev. Lett. **81**, 1003 (1998).
[3] K. A. Tanaka *et al.*, Phys. Plasmas **7**, 2014 (2000).
[4] P. A. Norreys *et al.*, Phys. Plasmas **7**, 3721 (2000).
[5] C. Ren *et al.*, Phys. Rev. Lett. **93**, 185004 (2004).
[6] R. B. Campbell *et al.*, Phys. Plasmas, **10**, 4169 (2003).
[7] Y. Sentoku *et al.*, Phys. Plasmas, **11**, 3083 (2004).
[8] R. J. Mason, Phys. Rev. Lett., **96**, 035001 (2006); Bull. Am. Phys. Soc. **50**, 139 (2005).
[9] R. Kodama *et al.*, Nature (London) **418**, 933 (2002); **412**, 798 (2001).
[10] T. Nakamura *et al.*, Phys. Plasmas **14**, 103105 (2007).
[11] H. Nagatomo *et al.*, J. Phys. IV **133**, 397 (2006).
[12] J. A. Stamper *et al.*, Phys. Rev. Lett. **26**, 1012 (1971).
[13] R. N. Sudan, Phys. Rev. Lett. **70**, 3075 (1993).
[14] H. B. Cai *et al.*, Phys. Rev. E **76**, 036403 (2007).
[15] F. Califano *et al.*, Phys. Rev. E **56**, 963 (1997).